Role of montmorillonite for enhancing fire retardancy of intumescent PLA

GAELLE FONTAINE*, ANTOINE GALLOS AND SERGE BOURBIGOT
ISP/UMET/UMR 8207
Ecole Nationale Supérieure de Chimie
Av Mendeleïev CS 90108
59652 Villeneuve d'Ascq Cedex France
* gaelle.fontaine@ensc-lille.fr

ABSTRACT

This work deals with the effect of an organomodified montmorillonite (OMMT, cloisite C30B) in intumescent PLA, which makes it nonflammable. The use of OMMT dramatically improves the fire properties of intumescent PLA in terms of limiting oxygen index (LOI) and heat release rate (HRR), which is almost zero. The part played by OMMT in the improvement of the FR performance was studied using a Microscale Combustion Calorimeter (MCC), solid-state NMR (^{13}C, ^{31}P and ^{27}Al) and specific set-up for temperature and swelling measurements in the char during fire test. It is shown that the clay increases the efficiency of the protective char by strongly limiting heat and mass transfer.

KEYWORDS: fire chemistry, polylactide, intumescence, montmorillonite.

INTRODUCTION

Polylactide or polylactic acid (PLA), is one of the most promising candidates for future developments regarding the substitution of petroleum-based polymers. PLA is biodegradable and is produced from non-fossil renewable natural resources by fermentation of polysaccharides or sugar, which are extracted from sugar beet or corn, by establishing a biological cycle with PLA biodegradation as well as photosynthesis fore. [1, 2] It is used in many applications such as packaging, tissue engineering, drug delivery [3] but increasingly its applications are from short term to long life applications such as composites, electronics, automotive, and household items which require fire retardant properties.

There have been numerous studies on improving the thermal stability and flame retardancy of PLA. Additive-type flame retardants, such as phosphorus-containing [4, 5] silicon-containing [6], or carbon-containing materials [7, 8], inorganic materials [9-11], and synergistic combinations [12, 13], are used in PLA. We have recently reported [14] the efficiency of a combination of ammonium polyphosphate (APP)/Melamine (Mel) as an intumescent system and organomodified montmorillonite (OMMT, cloisite C30B) as synergist. The flame retardancy of this system was dramatically enhanced relative to the neat PLA via an intumescent phenomenon and also due to the specific action of the synergist. However the mechanism was not examined and it is the purpose of this paper.. The mechanism of action will be investigated by analyzing samples prepared after representative times of combustion by solid state nuclear magnetic resonance (NMR), and by measuring the physical parameters of intumescence (expansion and heat gradient). Then a mechanism of action will be proposed, and the specific role of the synergist will be discussed.

EXPERIMENTAL

Materials and methods

PLA (number average molar mass = 74500 g/mol, residual monomer content = 0.18 %, D-isomer content = 4.3 %, melt flow index (190 °C, 2.16 kg) = 6.61 g/10 min and density: 1.25 g/cm3) was supplied by NatureWorks and dried overnight at 110 °C before use. Flame retardants (FRs): APP (Exolit AP 422, soluble fraction in water <1 wt.-%) in powder was supplied by Clariant (Knapsak, Germany). Melamine (99 %) was obtained from Aldrich. Montmorillonite (MMT) originated from Southern Clay Products, Inc. (Gonzales, TX – USA). The starting material, sodium-MMT, was commercially modified using methyl, tallow, bis-2-hydroxyethyl, quaternary ammonium chloride (Cloisite 30B).

The FRs were dried for 24 h at 80 °C before use.

Preparation of the samples

PLA/FR and PLA/FR/Cloisite: PLA was mixed with FRs (30 wt.-% loading) at 185 °C using a Brabender laboratory E350 mixer measuring head (roller blades, constant shear rate of 50 rpm) for 10 min. Regarding PLA/FR/Cloisite: PLA was melt-mixed with the nanoparticle and the FRs using the same protocol as described above. The loading of nanoparticle was 1.00 wt.-% with constant loading in FR/OMMT, i.e., 30 wt.-% [Table 1].

Table 1. Compositions and names of the formulations of PLA/Melamine/APP/ Cloisite at 30 wt.-% loading

PLA (wt.-%)	**FR Loading (wt.-%)**	Melamine (wt.-%)	APP (wt.-%)	OMMT C30B (wt.-%)	**Formulation Name**
100	**-**	-	-	-	**PLA**
70	**30**	5.00	25.00	0.00	**PLAMel5APP25**
70	**30**	4.83	24.17	1.00	**PLAMel5APP25C30B**

Fire testing

FTT: (Fire Testing Technology) A Mass Loss Calorimeter was used to carry out measurements on samples following the procedure defined in ASTM E 906. Our procedure involved exposing specimens measuring 100 mm x 100 mm x 3 mm in horizontal orientation. An external heat flux of 35 kW/m² was used for running the experiments. This flux corresponds to the common heat flux in a mild fire scenario. When measured at 35 kW/m², HRR is reproducible to within ± 10%. The data reported in this paper are the averages of three replicated experiments.

Microscale Combustion Calorimeter (MCC)**:** The fire-retardant capability to limit the release of combustible products was evaluated with a Microscale Combustion Calorimeter (MCC) supplied by Fire Testing Technology Ltd. Samples of about 5 mg were placed in open alumina pans and were degraded in a nitrogen atmosphere at a heating rate of 1 °C/s and a nitrogen flow of 80 cm^3/min. The decomposition gases were then burnt in a nitrogen/oxygen mixture (80 cm^3/min and 20 cm^3/min respectively) and the heat release rate was recorded as a function of temperature.

Temperature measurement: During mass-loss calorimeter experiments, K-type thermocouples were embedded in the samples (100 mm x 100 mm x 3 mm) at three different locations (Fig. 1). The first two are located at 1 and at 0.5 cm above the sample, and were located in the chars of the intumescent samples during the experiment, and after its swelling. The last one is inserted at the top surface of the sample. This setting permits the evaluation of the temperature gradients in the burning polymer.

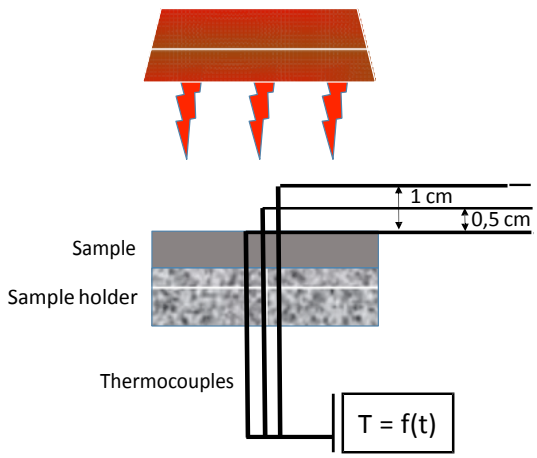

Fig. 1. Experimental set-up for measuring the temperature during a mass loss experiment using thermocouples

Swelling: In order to measure the swelling of intumescent samples (100 mm x 100 mm x 3 mm) during mass-loss calorimetry and link it to other parameters, the development of the char was monitored by an infrared camera (Fig. 2). The obtained images were then processed using image analysis software and the relative swelling was calculated.

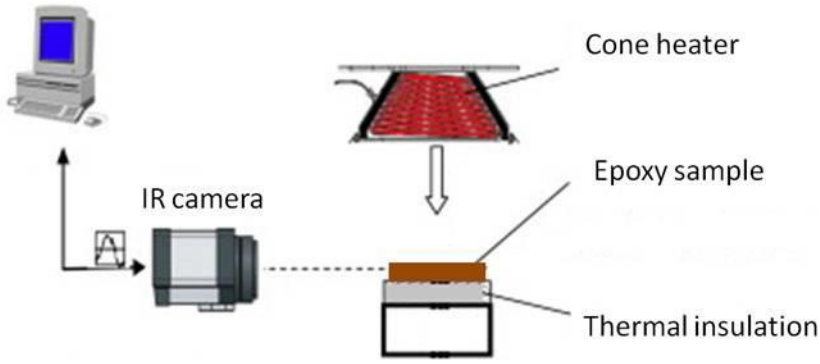

Fig. 2. Experimental set-up for measuring swelling during a mass loss experiment using infrared camera

Solid-state NMR

^{13}C NMR analyses were carried out on a Bruker Avance II 400 spectrometer equipped with a 4 mm probe and at the Larmor frequency of 100.63 MHz (9.4 T). Measurements were performed with cross-polarization and high power ^{1}H dipolar decoupling with MAS (magic angle spinning) at 10 kHz or 12.5 kHz. The contact time was set at 1 ms and the delay between scans was 5 s. Tetramethylsilane ($Si(CH_3)_4$) was used as a reference.

^{31}P NMR analyses were carried out on the same spectrometer as above. The Larmor frequency was 40.5 MHz (9.4 T). Measurements were performed with ^{1}H dipolar decoupling at 10 kHz in MAS conditions. Between the scans, a 120 s delay was used to ensure full relaxation of the nucleus. Phosphoric acid (H_3PO_4) in aqueous solution (85 %) was used as a reference.

^{27}Al NMR measurements were carried out on the same spectrometer as above at 24.5 MHz (9.4 T) with MAS of 15 kHz). The repetition time was fixed at 1 s due to the quick relaxation time of the quadripolar nucleus, and a minimum of 1024 scans was necessary to obtain a satisfactory signal to noise ratio. Al in aqueous solution ($Al(OH)_3$) was used as a reference.

RESULTS AND DISCUSSION

Reaction to fire

The fire behavior measured by cone calorimetry [14] is depicted in Fig. 3 and the associated parameters are summarized in Table 2. The pictures (Fig. 4) of the residues after mass loss experiments reveal the intumescence of the chars. Regarding the results, it appears that neat PLA exhibits a peak of heat released rate (pHRR) of 279 kW/m² whereas incorporation of 30 wt.-% of melamine and APP (ratio 1/5) result in a decrease of pHRR by 85 %. A synergistic effect is obtained when 1 % of intumescent FR system is substituted by 1 % of OMMT: the reduction is then about 90 %. Moreover a reduction of 82 % and 95 % of the total heat release (THR) is observed for PLAMel5APP25 and PLAMel5APP25C30B, respectively. During the experiment only a few flames were observed at the surface of the intumescent samples in contrast to neat PLA, which burned rapidly and with high flames. It is noteworthy that in the case of PLAMel5APP25C30B the sporadic flames extinguished spontaneously and quickly. Another important phenomenon is the increase of the time-to-ignition, which is observed for intumescent formulations (from 86 s for neat PLA to 110 s for FR PLA). Concerning the remaining mass after the experiment, it can be noted that both FR PLAs exhibit the same mass which represent 50 % of the starting mass. The residues of the samples after mass loss experiments are shown in Fig. 4. It can be observed that the chars are quite similar and exhibit a sponge-like structure.

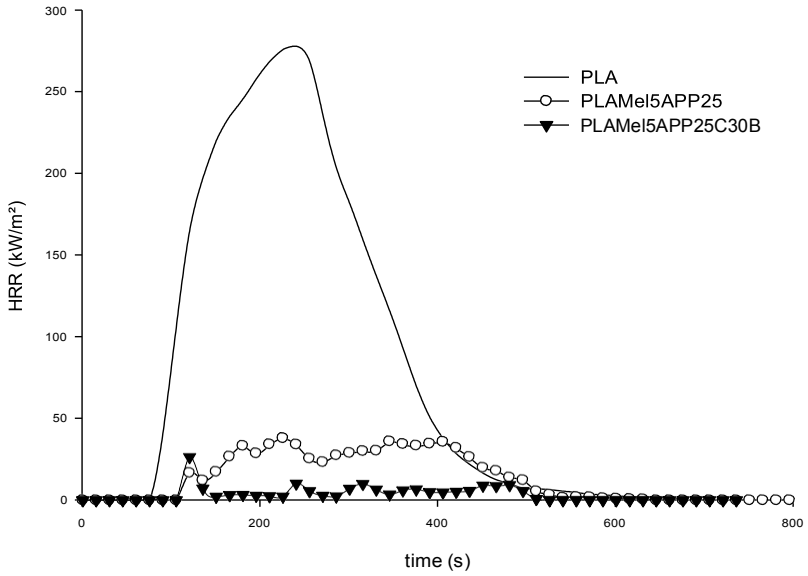

Fig. 3. Mass Loss experiment of PLA formulations at 35 kW/m^2

Table 2: Mass-loss calorimeter main parameters for PLA formulations

Sample	TI(s)	Residual weight (%)	pHRR (kW.m^{-2}) (% reduction)	THR (MJ.m^{-2}) (% reduction)
PLA	86	0	279	59.7
PLAMel5APP25	110	50	37 (-85 %)	10.7 (-82 %)
PLAMel5APP25C30B	110	50	29 (-90 %)	2.5 (-96 %)

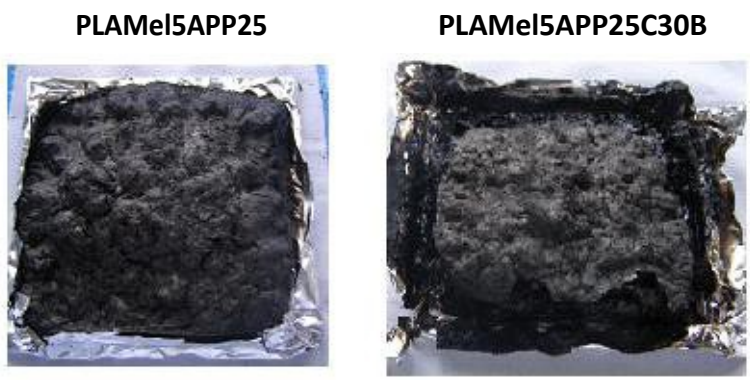

Fig. 4. Residual char of PLAMel5APP25 (left) and PLAMel5APP25C30B (right) after mass loss experiment at 35 kW/m²

These results indicate that we obtain very effective intumescent systems. Specific experiments should be done in order to elucidate the mechanisms involved during this fire scenario. Hereafter the experiments will be described and discussed. First, we investigated the potential chemical interactions; then, we studied the physical parameters governing the fire retardancy.

Chemical interactions

MCC [15, 16]: The heat released by the burning of combustible compounds and the temperatures at which they are released can be evaluated by MCC. In our case, this is used to determine if a flame retardant modifies the degradation pathway, evolving less flammable species (or a different composition), or acts through a condensed-phase mechanism. Only one main step is observed for all formulations, melamine, and APP, whereas for C30B its decomposition occurs in two steps under the conditions of the experiment (Fig. 5 and Table 3). The pHRR for PLA occurs at 368 °C and reaches 461 W/g. The combination of melamine and APP with or without C30B, does not really increase the temperature at which the pHRR occurs (370 °C and 360 °C) but it slightly decreases the peak by 33 % and 35 % for PLAMel5APP25 and PLAMel5APP25C30B, respectively. This reduction can be attributed to the substitution of PLA by a mixture of melamine, APP, and C30B, which exhibit low heat releases, i.e., 128 W/g for melamine, 20 W/g for APP and two peaks at 38 W/g and 50 W/g for C30B. With the aim of verifying this, the theoretical curve of PLAMel5APP25 (curves deduced from the linear combination of the MCC curves of the sole components) is compared with the experimental data (Fig. 5). It can be observed that there is no significant difference between them indeed they present the same peak of HRR (316 W/g) at similar temperature, i.e., 368 °C for the theoretical curve and 360 °C for the experimental one. This indicates that in this experiment no interactions between the components of the formulations are observed.

Our assumption is based on the particular design of PCFC in which 2 mg of sample is put in a pan and undergoes its thermal degradation at high heating rate like in TGA and where the evolving gases are then burnt in a combustor measuring HRR. In such a design, we do not believe that an efficient physical barrier could be formed and the decrease of pHRR observed in MLC due to the modification of HRR can only be due to the chemical changes of the evolving gases.

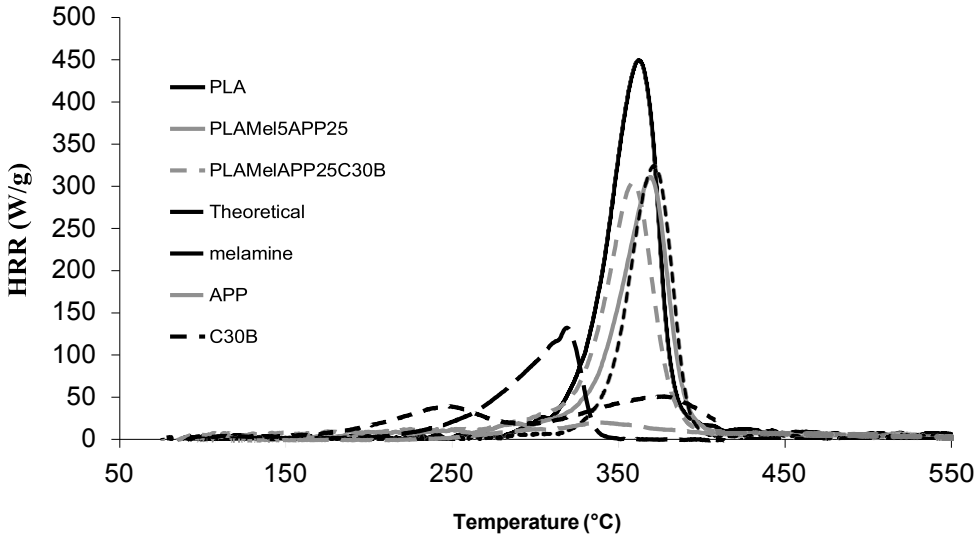

Fig. 5. MCC experiment of PLA formulations at 1 °C/s

Table 3. MCC main parameters for PLA formulations (Heating rate: 1 °C/s)

Formulation	Temp.@pHRR (°C)	pHRR (W/g) (% reduction)	THR ($kW.g^{-1}$)
PLA	368	461	31.1

PLAMel5APP25	370	308 (-33 %)	27.0 (-13 %)
PLAMel5APP25C30B	360	301 (-35 %)	27.2 (-12 %)
Melamine	320	128	13.8
APP	342	20	5.2
C30B	250 / 380	38 / 50	14.7

Solid state NMR: In order to detect potential chemical interactions between the components of each formulations occurring during the fire scenario, the samples were analyzed by solid state NMR at representative times deducted from mass loss calorimeter curves. These times are 0 s, 120 s, 180 s, 400 s and 800 s and are related to the reference (0 s), to the ignition (120 s), to the period after ignition (180 s), to the protection by the intumescent char (400 s) and finally, to the end of the heat release (800 s). Mass-loss calorimetry experiments were stopped at these characteristic times of the HRR curve and the resulting samples were analyzed.

The ^{13}C solid state NMR permits to evaluate the modification of the PLA matrix as a function of external heat flux. The NMR spectra for the two FR PLAs as a function of time are similar and only PLAMel5APP25C30B ones are presented (Fig. 6). At 0 s the spectrum exhibits three bands attributed to the three carbons in the PLA matrix: one for the ester function at 168ppm, one for the aliphatic at 69ppm and one for the methyl carbon at 16ppm. At 120 s, the signals are still observed (suggesting that the PLA is not (or not very much) degraded) but their shape is different: they are broader with less resolution indicating a higher disorder in PLA. After ignition (180 s) four signals are observed, i.e., three from PLA, and an additional broad band of low intensity from 160 ppm to 100 ppm, related to unsaturated carbon (double bond and aromatic carbons) [17, 18]: this indicates the beginning of the carbonization. Then, at 400 s only two broad bands can be distinguished, the formation of the char is observed by the band between 160 ppm and 100 ppm whereas the second band centered at 30 ppm is attributed to aliphatic carbons (-CH, -CH_2, -CH_3) [18, 19]. At the end of the experiment (800 s) the two broad bands are still present characterizing the char. There are also two bands from the PLA matrix detected; this is due to the heterogeneous sample and the sampling. The sample that has to be analyzed is taken from the top of the char but at the end of the mass loss experiment this becomes less dense so we need to go deeper and closer to the bottom of the sample where residual non-degraded PLA remains (this suggests therefore that the protection is efficient enough to prevent the full degradation of PLA).

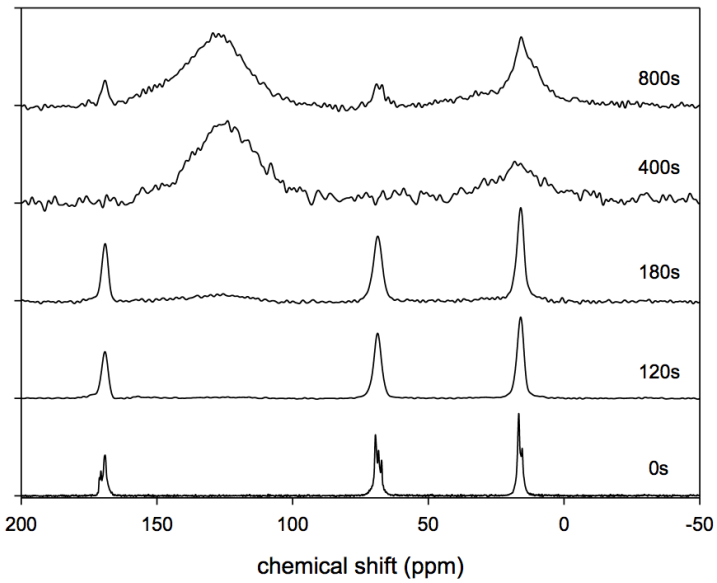

Fig. 6. 13C CP-DD-MAS NMR spectra of the residues of PLAMelAPPC30B formulation at different mass- loss experiment times

Since the samples contain ammonium polyphosphate, this is useful to follow the evolution and interactions with other chemicals if any of the phosphorus species by solid state ^{31}P NMR. As this was done for ^{13}C NMR the PLAMel5APP25 and PLAMel5APP25C30B samples were analyzed at the same characteristic times.

Regarding the sample without OMMT (Fig. 7), at 0 s, the signals observed at -21,7 ppm and -22.4 ppm are representative of the chemical surrounding of phosphorus in ammonium polyphosphate [20, 21]. Before ignition (120 s) three additional signals appear at 0 ppm, -11 ppm and -25 ppm. The one at 0 ppm is characteristic of orthophosphates linked to aliphatic carbons and/or orthophosphates adsorbed in intumescent structure in Q^0. Concerning the signal at -11 ppm it is characteristic of Q^1 structure in pyrophosphate [20]. The broad peak at -25 ppm is attributed to Q^2 type phosphate probably in polyphosphoric acid [22]. While the ignition occurs (180 s) the same signals as at 120 s are observed but they are broader. This broadening can be explained by a less organized structure. For 400 s and 800 s the recorded signals are very similar and are representative to Q^0 and Q^1 PO_4 units in ortho and pyrophosphates.

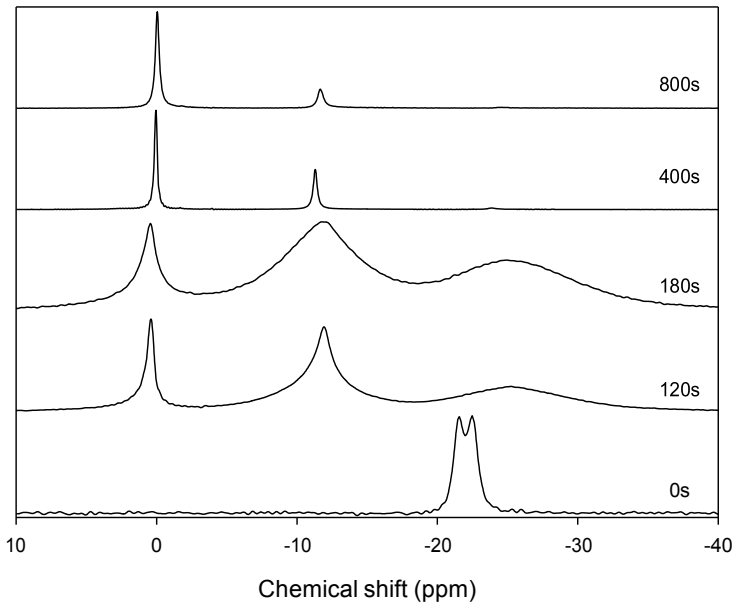

Fig. 7. ^{31}P NMR spectra of the mass-loss calorimeter residues of PLAMelAPP

The solid state ^{31}P NMR recorded spectra for PLAMel5APP25C30B are presented in Fig. 8 and they are not very different than those of PLAMel5APP25. The main differences are i) the broad peak at -25 ppm attributed to Q^2 type phosphate appeared later when OMMT is incorporated, i.e., at 180 s instead of 120 s for PLAMel5APP25 and ii) a broad peak at -2ppm is observed at 800 s assigned to orthophosphates (Q^0) [18][23].

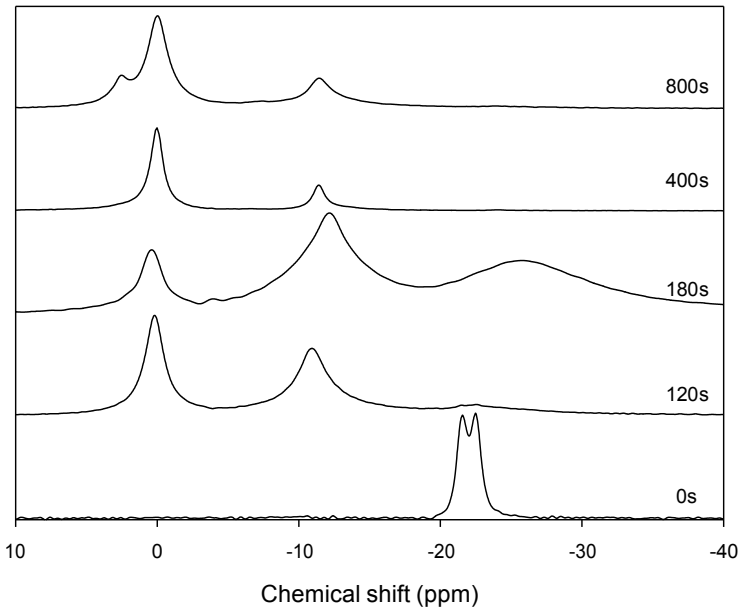

Fig. 8. ^{31}P NMR spectra of the mass-loss calorimeter residues of PLAMelAPPC30B

Since we investigated the mechanism of action of the intumescent formulations based on APP and OMMT, it is of interest to run ^{27} Al solid state NMR (Fig. 9). Indeed, it was already observed interactions between APP and C30B [24]. The room temperature PLAMel5APP25C30B spectrum had one band centered at 8 ppm, which can be assigned to Al in octahedral coordination [25, 26]. Another signal from the OMMT should be observed at 68 ppm corresponding to Al in tetrahedral coordination [25-27] but since the amount of OMMT is very low, that one is not observed. At 120 s the spectrum presents two peaks, a broad one at -14ppm and second one which is low intense and broad at 8 ppm. The latter corresponds to neat OMMT but because of thermal degradation the structure is less organized. The band around - 14 ppm was observed on all spectra which can be assigned to octahedral [AlO_6] units [28]. It is interesting to note that the peak position was shifted to higher fields. This is because of the presence of phosphorous within the second sphere of coordination. This phosphorus has a marked effect upon the peak position of AlOx units; which shifts from +10 for Al[OAI]$_6$ to -14 ppm for Al[OP]$_6$ [28-30]. This shows, therefore, that the clay can react with APP to form aluminophosphates. This result agrees with the work of Clearfield et al., [31] which showed that montmorillonite was completely collapsed by phosphate in solution. This signal was not observed in NMR ^{31}P with our experimental conditions because of the low content of clay (in NMR ^{31}P the chemical shift of an aluminophosphate lies between – 25 and - 35 ppm).

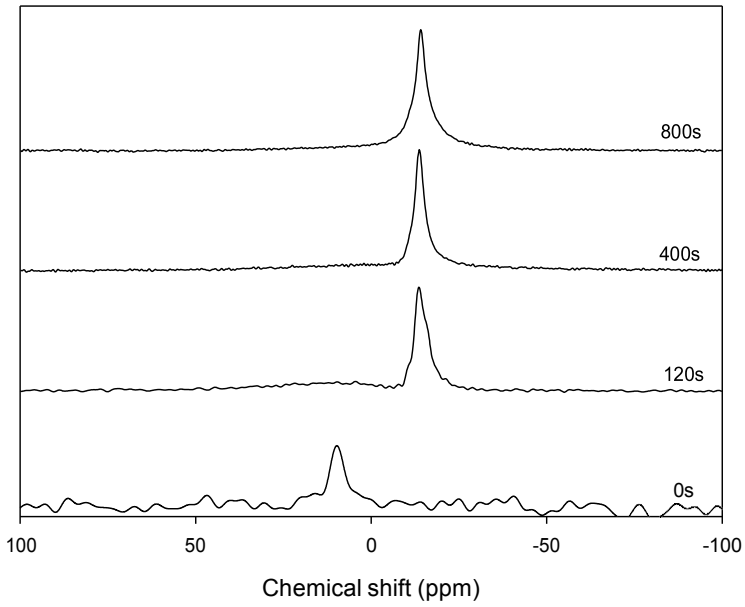

Fig. 9. [27] Al spectra of the mass loss calorimeter residues of PLAMelAPPC30B

Dynamic evolution

Intumescent formulations act by forming an insulating layer at the surface of the materials. Therefore, this part is dedicated to the heat gradient and expansion of the char in order to characterize the protection provided by the intumescent char. The layer formed, apart from limiting fuel flows between the inside of the material and the environment, should act as a heat insulator. Therefore, thermocouples recording the temperatures during the test were inserted in the sample at three different locations. Simultaneously, the swelling of the sample was recorded by an infrared camera associated to an image analysis protocol. The Fig. 10 and Fig. 11 present the temperature measured at different locations (in the sample, in the char at 0.5 cm and 1 cm of the bottom of the sample) in the PLAMel5APP25 and PLAMel5APP25C30B, respectively. It should be noticed that the measured temperature is representative when thermocouple is embedded in the polymer or in the char. It is observed for PLAMel5APP25 that the temperatures increase quickly for the 100 first seconds for thermocouple in the sample and the one at 0.5cm, for the one at 1cm the increase is observed up to 200 s. Then the temperatures raise a pseudo steady state at 320 °C (in the sample), 400 °C (0.5cm) and 470 °C (1cm) representing a temperature gradient of 150 °C.

The same phenomenon is observed for the FR formulation containing C30B, i.e., the temperatures increase quickly then a steady state is observed. The temperatures of the plateaus are 320 °C, 360 °C and 430 °C for the thermocouple in the sample, at 0.5 cm and 1 cm, respectively. In this case the temperature gradient is 110 °C and is less than PLAMel5APP25 previously studied. The OMMT containing formulation permits to obtain a lower temperature for the higher thermocouple, i.e, 430 °C vs. 470 °C for PLAMel5APP25.

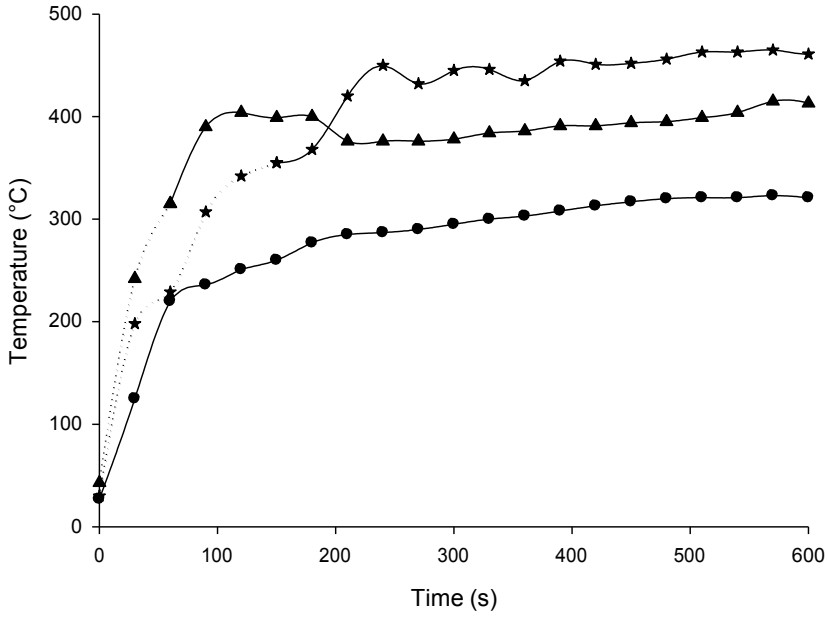

Fig. 10. Temperature measurement as a function of time in the char of PLAMelAPP formulation during mass loss experiment in the material (●), at 0.5cm from the bottom (▲), at 1.0 cm from the bottom (★) the dash line indicates that the thermocouple is in the air

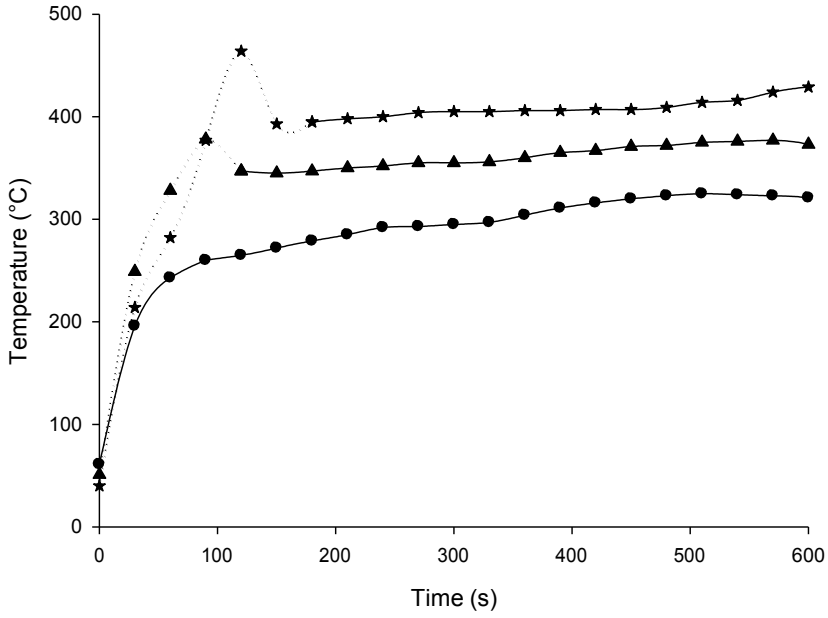

Fig. 11. Temperature measurement as a function of time in the char of PLAMelAPPC30B formulation during mass loss experiment in the material (●), at 0.5cm from the bottom (▲), at 1.0 cm from the bottom (★) the dot line indicates that the thermocouple is in the air

It was demonstrated that the swelling rate plays an important role in the insulated protection [32]. Fig. 12 shows the swelling of intumescent systems as a function of time. It is observed that the swelling rate of the two formulations exhibit the same shape presenting two main-step swelling. The first one is observed between 0 s and 250 s where the swelling is about 300 % for PLAMel5APP25 and 200 % for PLAMel5APP25C30B. Thus, the swelling rate of the latter is lower than that for PLAMel5APP25. After a plateau, there is second swelling from 200 % to 300 % for the formulation with C30B and from 300 % to 450 % without C30B. This difference of swelling can be due to the viscosity of the sample during swelling [33].

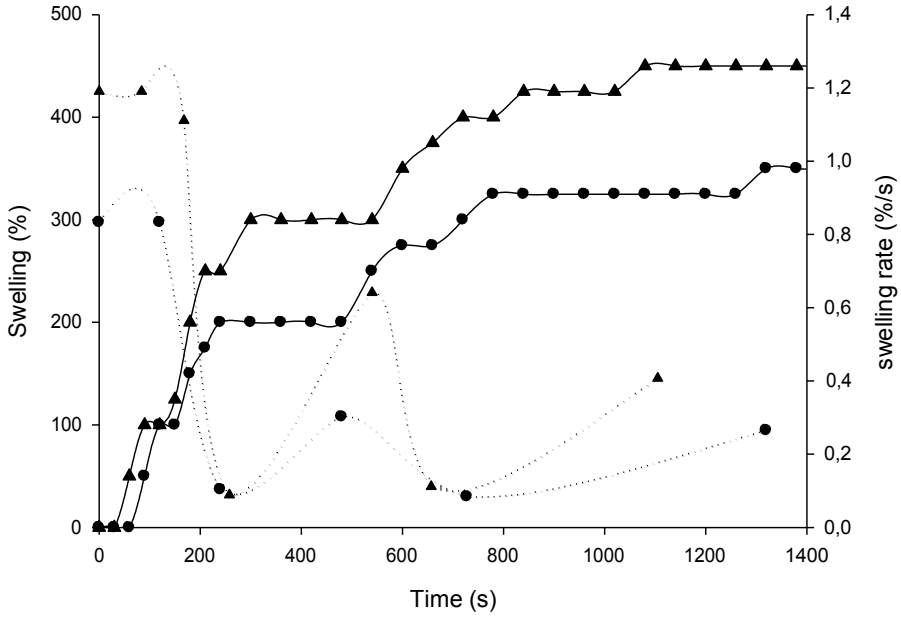

Fig. 12. Swelling (plain) and swelling rate (dot) as a function of time for PLAMelAPP formulation (▲) and PLAMelAPPC30B formulation (●)

MECHANISM OF ACTION AND CONCLUSION

This paper has shown the superior performance of intumescent PLA which is nonflammable (under mass loss calorimetry experiment at 35 kW/m²). The fire retardancy is obtained by intumescence using a combination of Melamine and APP in appropriate ratio (1 to 5) and with OMMT providing synergistic effect. The mechanism of action was carefully investigated by means specific experiments like solid state NMR (^{13}C, ^{31}P, ^{27}Al), expansion of the char and heat gradient in the intumescent coating during calorimetric experiment (MLC). These specific experiments permit to propose a mechanism for the fire retardancy and for the effect of the OMMT.

In the clay containing formulation, we have shown that clay reacts with the APP and forms aluminophosphate species. These species can thermally stabilize the structure of the char and permit to obtain a more cohesive char. A decrease of the swelling rate and of the expansion is also observed in the OMMT based formulation. Moreover the temperature measured by the higher thermocouple is lower in PLAMelAPPC30B than in the formulation without OMMT

The role played by the clay in the improvement of the FR performance is proposed as follows: the OMMT permits to obtain a better protection by an intumescent and more insulating char (less swelling but lower temperature). The char also limits the 'fuel' release due to its better cohesion. This limitation of fuel released is a consequence of the diminution of the HRR since there is less fuel to feed the flame and the

sporadic flames observed extinguish spontaneously and quickly. This intumescent PLA becomes then nonflammable.

REFERENCES

[1] Drumright R.E., Gruber P.R., Henton D.E., (2000) Polylactic acid technology, Advanced Materials 12: 1841-1846, 10.1002/1521-4095(200012)12:23<1841::AID-ADMA1841>3.0.CO;2-E

[2] Platt D.K., Limited R.T., Biodegradable Polymers: Market Report. Rapra Technology Limited 2006, p. 158.

[3] Gupta A.P., Kumar V., (2007) New emerging trends in synthetic biodegradable polymers - Polylactide: A critique, European Polymer Journal 43: 4053-4074, 10.1016/j.eurpolymj.2007.06.045

[4] Wang D.Y., Song Y.P., Lin L., Wang X.L., Wang Y.Z., (2011) A novel phosphorus-containing poly(lactic acid) toward its flame retardation, Polymer 52: 233-238, 10.1016/j.polymer.2010.11.023

[5] Tao K., Li J., Xu L., Zhao X., Xue L., Fan X., Yan Q., (2011) A novel phosphazene cyclomatrix network polymer: Design, synthesis and application in flame retardant polylactide, Polymer Degradation and Stability 96: 1248-1254, 10.1016/j.polymdegradstab.2011.04.011

[6] Bourbigot S., Duquesne S., Fontaine G., Bellayer S., Turf T., Samyn F., (2008) Characterization and Reaction to Fire of Polymer Nanocomposites with and without Conventional Flame Retardants, Molecular Crystals and Liquid Crystals 48610.1080/15421400801921983

[7] Bourbigot S., Fontaine G., Gallos A., Gérard C., Bellayer S. Functionalized-carbon multiwall nanotube as flame retardant for polylactic acid. In: Wilkie CA, Morgan AB, Nelson GL (eds) Fire and Polymers V - Materials and Concepts for Fire Retardancy American Chemical Society, Washington, DC, (2009), p 25-34

[8] Murariu M., Dechief A.L., Bonnaud L., Paint Y., Gallos A., Fontaine G., Bourbigot S., Dubois P., (2010) The production and properties of polylactide composites filled with expanded graphite, Polymer Degradation and Stability 95: 889-900, 10.1016/j.polymdegradstab.2009.12.019

[9] Murariu M., Bonnaud L., Yoann P., Fontaine G., Bourbigot S., Dubois P., (2010) New trends in polylactide (PLA)-based materials: "Green" PLA-Calcium sulfate (nano)composites tailored with flame retardant properties, Polymer Degradation and Stability 95: 374-381,

[10] Yanagisawa T., Kiuchi Y., Iji M., (2009) Enhanced flame retardancy of polylactic acid with aluminum tri-hydroxide and phenolic resins, Kobunshi Ronbunshu 66: 49-54, 10.1295/koron.66.49

[11] Hapuarachchi T.D., Peijs T., (2010) Multiwalled carbon nanotubes and sepiolite nanoclays as flame retardants for polylactide and its natural fibre reinforced composites, Composites Part A: Applied Science and Manufacturing 41: 954-963, 10.1002/app.30783; 10.1016/j.polymdegradstab.2009.12.019

[12] Wang X., Xuan S., Song L., Yang H., Lu H., Hu Y., (2011) Synergistic Effect of POSS on Mechanical Properties, Flammability, and Thermal Degradation of Intumescent Flame Retardant Polylactide Composites, Journal of Macromolecular Science, Part B 51: 255-268, 10.1080/00222348.2011.585334

[13] Zhu H., Zhu Q., Li J., Tao K., Xue L., Yan Q., (2011) Synergistic effect between expandable graphite and ammonium polyphosphate on flame retarded polylactide, Polymer Degradation and Stability 96: 183-189, http://dx.doi.org/10.1016/j.polymdegradstab.2010.11.017

[14] Fontaine G., Bourbigot S., (2009) Intumescent polylactide: A nonflammable material, Journal of Applied Polymer Science 113: 3860-3865, 10.1002/app.30379

[15] Lyon R.E., Walters R.N., Stoliarov S.I., (2007) Screening flame retardants for plastics using microscale combustion calorimetry, Polymer Engineering and Science 47: 1501-1510, 10.1002/pen.20871

[16] Lyon R.E., Walters R.N., (2004) Pyrolysis combustion flow calorimetry, Journal of Analytical and Applied Pyrolysis 71: 27-46, http://dx.doi.org/10.1016/S0165-2370(03)00096-2

[17] Camino G., Costa L., Clouet G., Chiotis A., Brossas J., Bert M., Guyot A., (1984) Thermal degradation of phosphonated polystyrenes: Part 1-Chain end condensation, Polymer Degradation and Stability 6: 105-121,

[18] Maciel G.E., Bartuska V.J., Miknis F.P., (1979) Characterization of organic material in coal by proton-decoupled 13C nuclear magnetic resonance with magic-angle spinning, Fuel 58: 391-394,

[19] Maciel G.E., Sullivan M.J., Petrakis L., Grandy D.W., (1982) 13C Nuclear magnetic resonance characterization of coal macerals by magic-angle spinning, Fuel 61: 411-414,

[20] Duncan T.M., Douglas D.C., (1984) On the 31P chemical shift anisotropy in condensed phosphates, Chemical Physics 87: 339-349,
[21] Van Wazer J.R., Callis C.F., Shoolery J.N., Jones R.C., (1956) Principles of phosphorus chemistry. II. Nuclear magnetic resonance measurements, Journal of the American Chemical Society 78: 5715-5726,
[22] Walter G., Hoppe U., Vogel J., Carl G., Hartmann P., (2004) The structure of zinc polyphosphate glass studied by diffraction methods and 31P NMR, Journal of Non-Crystalline Solids 333: 252-262, 10.1016/j.jnoncrysol.2003.12.054
[23] Kovalev I.V., Kovaleva N.O., (2011) Organophosphates in agrogray soils with periodic water logging according to the data of 31P NMR spectroscopy, Eurasian Soil Science 44: 29-37, doi 10.1134/S1064229311010066
[24] Bourbigot S., Le Bras M., Dabrowski F., Gilman J.W., Kashiwagi T., (2000) PA-6 clay nanocomposite hybrid as char forming agent in intumescent formulations, Fire and Materials 24: 201-208, 0.1002/1099-1018(200007/08)24:4<201::AID-FAM739>3.0.CO;2-D
[25] Van Eck E.R.H., Kentgens A.P.M., Kraus H., Prins R., (1995) A solid state double resonance NMR investigation of phosphorus-impregnated γ-Al2O3, Journal of Physical Chemistry 99: 16080-16086,
[26] Duffy S.J., vanLoon G.W., (1995) Investigations of aluminum hydroxyphosphates and activated sludge by 27Al and 31P MAS NMR, Can J Chem 73: 1645-1659, 10.1139/v95-204
[27] Lookman R., Grobet P., Merckx R., Vlassak K., (1994) Phosphate sorption by synthetic amorphous aluminum hydroxides: a 27Al and 31P solid-state MAS NMR spectroscopy study, Eur J Soil Sci 45: 37-44, 10.1111/j.1365-2389.1994.tb00484.x
[28] Mueller D., Berger G., Grunze I., Ladwig G., Hallas E., Haubenreisser U., (1983) Solid-state high-resolution aluminum-27 nuclear magnetic resonance studies of the structure of calcium oxide-aluminum oxide-phosphorus pentoxide glasses, Phys Chem Glasses 24: 37-42,
[29] Müller D., Gessner W., Behrens H.J., Scheler G., (1981) Determination of the aluminium coordination in aluminium-oxygen compounds by solid-state high-resolution 27AI NMR, Chemical Physics Letters 79: 59-62,
[30] Dupree R., Holland D. (1989) MAS NMR: a new spectroscopic technique for structure determination in glasses and ceramics. Chapman and Hall, pp 1-40
[31] Clearfield A., Kuchenmeister M., (1992) Pillared layered materials, ACS Symp Ser 499: 128-144, 10.1021/bk-1992-0499.ch010
[32] Gérard C. (2011) Contribution of nanoparticles to the flame retardancy of expoy resins. Université des sciences et technologies de Lille
[33] Jimenez M., Duquesne S., Bourbigot S., (2006) Characterization of the performance of an intumescent fire protective coating, Surface and Coatings Technology 201: 979-987, 10.1016/j.surfcoat.2006.01.026